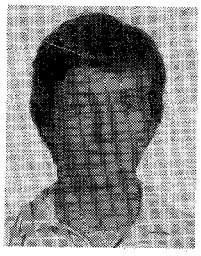

David T. Borup was born in Boise, ID, on October 24, 1958. He received the B.S. degree in mathematics from the College of Idaho, Caldwell, ID, in 1981. He is presently studying toward the Ph.D. degree at the University of Utah, Salt Lake City, where he has been working on numerical methods for microwave dosimetry.

✚

Om P. Gandhi (S'57–M'58–SM'65–F'79) received the B.Sc. (honors) degree in physics from Delhi University, Delhi, India, and the M.S.E. and Sc.D. degrees in electrical engineering from the University of Michigan, Ann Arbor.

He is a professor of Electrical Engineering at the University of Utah, Salt Lake City. He is an author or coauthor of one technical book and over 140 journal articles on microwave tubes, solid-state devices, and electromagnetic dosimetry and has recently written the textbook *Microwave Engineering and Applications* published by Pergamon Press. He has done pioneering work in quantifying the electromagnetic absorption in man and animals including the whole-body and part-body resonance conditions—work that formed an important basis for the new ANSI C95 recommended safety level with respect to human exposure to RF fields. He has been a principal investigator on over a dozen federally funded research projects since 1970, and serves or has served as a Consultant to several government agencies and private industries.

Dr. Gandhi received the Distinguished Research award of the University of Utah for 1979–1980 and a special award for "Outstanding Technical Achievement" from the Institute of Electrical and Electronics Engineers, Utah Section, in 1975. He edited a "*Proceedings of the IEEE*" Special Issue (January 1980) on Biological Effects and Medical Applications of Electromagnetic Energy. In addition to his membership on numerous national professional committees, he has been a Member of the Board of Directors of the Bioelectromagnetics Society and serves on the Editorial Board of its journal "Bioelectromagnetics." He is currently serving as the Chairman of the IEEE Committee on Man and Radiation (COMAR). His name is listed in *Who's Who in Engineering*, and *Who's Who in Technology Today*.

Characteristics of Transmission Lines with a Single Wire for a Multiwire Circuit Board

HISASHI SHIBATA AND RYUITI TERAKADO

Abstract—**This paper presents the characteristic impedance Z_0 and the phase velocity v_p of transmission lines with a single wire for a multiwire circuit board (MWB) under the quasi-TEM wave approximation. The characteristics are discussed for each of three investigated structures as: (I)$H = h + r$, (II)$H = h$, and (III)$H = h - r$, where r, h, and H are the radius of the wire, the thickness of the dielectric (adhesive layer), and the distance from the ground plane to the center of the wire, respectively. A charge simulation method is used for the calculation of the parameters. Z_0 and v_p are presented in graphical form for adhesive relative dielectric constants ϵ^* of 1.0, 2.65, and 5.0 as a function of r/h. An approximate formula of Z_0 for the structure of case (II) with $\epsilon^* = 5.0$ is also presented.**

I. Introduction

THE MULTIWIRE circuit board (MWB) [1]–[4] has become a center of attraction as a new technology for the printed wiring board. The technology is simple to design and offers the possibility of high interconnection density. The manufacturing process is described in [4]. The cross section of an MWB with a single wire is shown in Fig. 1. The electrical characteristics of the structure shown in Fig. 1 are discussed in [2], [3]. In general, the experiment based on the propagation delay [5] is used to obtain the characteristic impedance. Therefore, it is very important to present, theoretically, the design data for the impedance of the structure shown in Fig. 1.

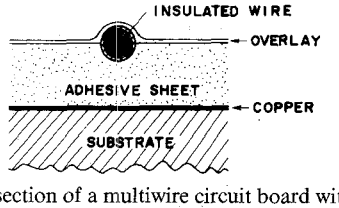

Fig. 1. Cross section of a multiwire circuit board with a single wire.

For this purpose, we consider three structures as shown in Fig. 2. The configurations of the structures are specified by the parameters r/h and H, where r, h, and H are the radius of the wire, the thickness of dielectric (adhesive) sheet, and the distance from the ground plane to the center of the wire, respectively. Because the coating of wire and the overlay in Fig. 2 have been neglected, the structures of Fig. 1 and Fig. 2(a) are different in a strict sense. However, when the thickness of the overlay is thin, the structure of Fig. 2(a) is, approximately, a good model for the analysis

Manuscript received April 22, 1983; revised November 2, 1983.

H. Shibata is with the Department of Electrical Engineering, Ibaraki Technical College, Katsuta, Ibaraki, 312 Japan.

R. Terakado is with the Department of Electrical Engineering, Faculty of Engineering, Ibaraki University, Hitachi, Ibaraki, 316 Japan.

0018-9480/84/0400-0360$01.00 ©1984 IEEE

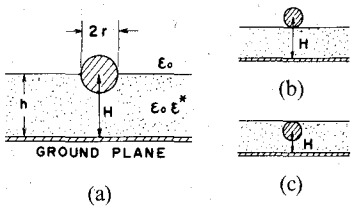

Fig. 2. Three structures for the analysis of the structure shown in Fig. 1. (a) $H = h$. (b) $H = h + r$. (c) $H = h - r$.

of the structure shown in Fig. 1. Furthermore, it is significant to analyze the structures of Fig. 2(b) and (c) because these states of wire may be taken by the conditions of the wiring and the thermal press. The structure shown in Fig. 2(b) has been reported in [5]–[9]. However, the characteristics of the structures shown in Fig. 2(a) and (c) have not been published.

Lines with a conductor of finite thickness involving two-dielectric layers can be analyzed by using an integral-equation method [10]–[13]. In the present work, the Green's function [10], [11] which already satisfies the boundary condition on the dielectric interface, is applied to a charge simulation method [14], [15] for computations of the line capacitance. The capacitances of the line without adhesive calculated using this method are in good agreement with theoretical values [9]. Using the quasi-TEM assumptions, the values of line capacitance are used to calculate the characteristic impedance and the phase velocity, which are presented in graphical form for each of the structures shown in Fig. 2. The graphs are presented for adhesive relative dielectric constants ϵ^* of 1.0 (air), 2.65, and 5.0 (epoxy resin), and a range of r/h values. An approximate formula of the impedance of the structure shown in Fig. 2(a) with the adhesive of $\epsilon^* = 5.0$ is also presented by employing the calculated results. Comparing the values of the present formula with experimental measurements [3] shows good agreement.

II. Calculation of Capacitance

We use a charge simulation method [14], [15] in calculating the line capacitances of the structures shown in Fig. 2. In this method, the distributed charges on the wire surface are equivalently replaced by the discrete fictitious line charges in the wire. The practical application of the method to the structures of Fig. 2 is shown in Fig. 3. In Fig. 3, the line charges and the contour points are equally arranged on the circles with radius r_q and r, respectively. It is now assumed that the coordinates of the charge points and the contour points are represented by (x_j, y_j) and (x_i, y_i), respectively. Because the line charges and the contour points are arranged symmetrically with respect to the x-axis, as shown in Fig. 3, we have

$$x_k = H + R\cos\frac{\pi}{n-1}(k-1), \qquad R = \begin{cases} r \text{ for } k = i \\ r_q \text{ for } k = j \end{cases}$$

$$y_k = R\sin\frac{\pi}{n-1}(k-1), \qquad k = i, j = 1,2,3,\cdots,n \quad (1)$$

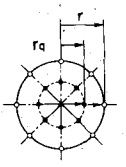

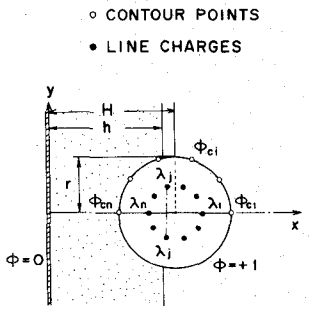

Fig. 3. Arrangement of the contour points on the wire surface and the line charges in the wire.

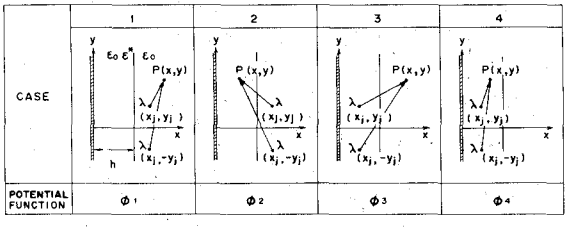

Fig. 4. Potential function at point $P(x, y)$.

where n is the number of pairs of line charges at the points (x_j, y_j) and $(x_j, -y_j)$.

For analysis based on the above method, we need the potential function at the point $P(x, y)$ for each of the four cases shown in Fig. 4. In Fig. 4, λ is the magnitude of line charge at the source points. The potential function in the presence of both the dielectric interface and the ground plane, as shown in Fig. 4, is derived using the method of images [10], [11]. The potential at P is given by

$$\Phi_1(x, y|x_j, \pm y_j) = \frac{\lambda}{4\pi\epsilon_0}\left[-K\ln\frac{(x+x_j-2h)^2+(y-y_j)^2}{(x-x_j)^2+(y-y_j)^2} \cdot \frac{(x+x_j-2h)^2+(y+y_j)^2}{(x-x_j)^2+(y+y_j)^2} + (1-K^2) \cdot \sum_{m=0}^{\infty} K^m \ln\frac{(x+x_j+2mh)^2+(y-y_j)^2}{(x-x_j)^2+(y-y_j)^2} \cdot \frac{(x+x_j+2mh)^2+(y+y_j)^2}{(x-x_j)^2+(y+y_j)^2} \right],$$

$$\text{for } x \geq h, x_j \geq h \quad (2a)$$

$$\phi_2(x, y|x_j, \pm y_j) = \frac{\lambda(1-K)}{4\pi\epsilon_0\epsilon^*} \sum_{m=0}^{\infty} K^m \ln \frac{(x+x_j+2mh)^2+(y-y_j)^2}{(x-x_j-2mh)^2+(y-y_j)^2} \cdot \frac{(x+x_j+2mh)^2+(y+y_j)^2}{(x-x_j-2mh)^2+(y+y_j)^2}, \quad \text{for } 0 \leqslant x \leqslant h, x_j \geqslant h \quad (2b)$$

$$\phi_3(x, y|x_j, \pm y_j) = \frac{\lambda(1+K)}{4\pi\epsilon_0} \sum_{m=0}^{\infty} K^m \ln \frac{(x+x_j+2mh)^2+(y-y_j)^2}{(x-x_j+2mh)^2+(y-y_j)^2} \cdot \frac{(x+x_j+2mh)^2+(y+y_j)^2}{(x-x_j+2mh)^2+(y+y_j)^2}, \quad \text{for } x \geqslant h, 0 < x_j \leqslant h \quad (2c)$$

$$\phi_4(x, y|x_j, \pm y_j) = \frac{\lambda}{4\pi\epsilon_0\epsilon^*}\left[\ln \frac{(x+x_j)^2+(y-y_j)^2}{(x-x_j)^2+(y-y_j)^2} \cdot \frac{(x+x_j)^2+(y+y_j)^2}{(x-x_j)^2+(y+y_j)^2} + \sum_{m=1}^{\infty} K^m \ln \frac{\left[(x+x_j-2mh)^2+(y-y_j)^2\right]\left[(x+x_j+2mh)^2+(y-y_j)^2\right]}{\left[(x-x_j+2mh)^2+(y-y_j)^2\right]\left[(x-x_j-2mh)^2+(y-y_j)^2\right]} \cdot \frac{\left[(x+x_j-2mh)^2+(y+y_j)^2\right]\left[(x+x_j+2mh)^2+(y+y_j)^2\right]}{\left[(x-x_j+2mh)^2+(y+y_j)^2\right]\left[(x-x_j-2mh)^2+(y+y_j)^2\right]}\right], \quad \text{for } 0 \leqslant x \leqslant h, 0 < x_j \leqslant h \quad (2d)$$

where

$$K = \frac{1-\epsilon^*}{1+\epsilon^*} \text{ is the image coefficient [10].}$$

In 2(a)–(d), ϵ_0 and ϵ^* are the permittivity of a vacuum and the relative dielectric constant of the adhesive layer, respectively. Because the potential is separated into four parts according to the location of the point of observation and the location of the line charge, we have to use them properly. For instance, ϕ_1 is used for the analysis of the structure of Fig. 2(b), and ϕ_4 is used for the structure of Fig. 2(c). For the structure of Fig. 2(a), not only are ϕ_1 and ϕ_4 used, but ϕ_2 and ϕ_3 are used as well. Furthermore, for the line charge at $y = 0$, we have to use the potential function as

$$\frac{1}{2}\phi_s(x, y|x_j, 0), \quad \begin{matrix}(s=1,2,3,4)\\(j=1 \text{ and } n)\end{matrix}. \quad (3)$$

The number of repetitions until termination for 2(a)–(d) in the practical computation is shown in the following section.

In the charge simulation method, the magnitudes of the line charges $\lambda_j (j=1,2,\cdots,n)$ are determined [14] by using the superposition of the potential $\phi_{ci} (i=1,2,\cdots,n)$ at every contour point and by solving the system of n linear equations for n line charges under the boundary condition, $\phi_{ci}=1$. Thus, the line capacitance C per unit length is obtained as

$$C = \lambda_1 + \lambda_n + 2\sum_{j=2}^{n-1} \lambda_j. \quad (4)$$

In the following section, the accuracy of the capacitance will be shown in relation to the potential error on the wire surface for various r_q/r ratios.

III. Accuracy of the Method

In this section, the relation among the capacitance error, the potential error on the wire surface, the number of charges, and the arrangement of charges are discussed. As a premise of the discussion, the condition

$$\phi_s(m+1) - \phi_s(m) \leqslant 10^{-10}, \quad (s=1,2,3,4) \quad (5)$$

is used as the criteria for terminating equations 2(a)–(d), which have been presented in the form of the infinite series. Also, the double precision computation for a digital computer is used. Under the condition of (5), the number of terms in the summation m for cases of $\epsilon^* = 2.65$ and $\epsilon^* = 5.0$ are about 30 and 60, respectively, for practical applications. Of course, the number m lessens if we use a less stringent condition for the termination.

Firstly, we compare the values of capacitance using the method based on (4) with the theoretical values [9], for the lines with $\epsilon^* = 1.0$. The comparison is shown in Fig. 5. Fig. 5(a) shows the values of the function F and the capacitance errors versus r_q/r. The evaluated function F for the potential error on the conductor surface has been defined as follows by Murashima *et al.* [17]:

$$F = \sqrt{\left(\sum_{i=1}^{M} E_i^2\right)\Big/ M}. \quad (6)$$

In (6), M is the number of check points which are placed on the middle point of the adjacent contour points, and E_i is the difference between the potential on the check point and the given boundary potential. This evaluation [16], [17]

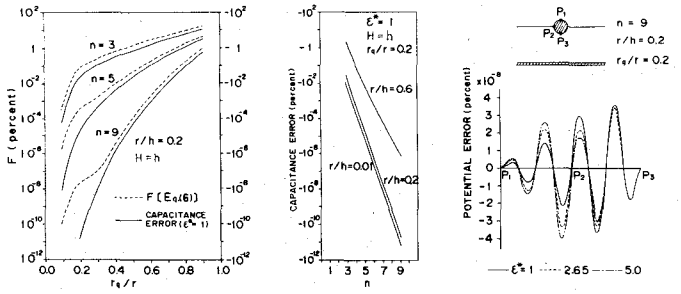

(a) (b) (c)

Fig. 5. Relation among the potential error on the wire surface, the capacitance error, the arrangement of the charges, and the number of charges. (a) Values of the evaluated function F and the capacitance error versus r_q/r for various n, (b) capacitance error versus n for various r/h ratios, (c) potential error on the wire surface.

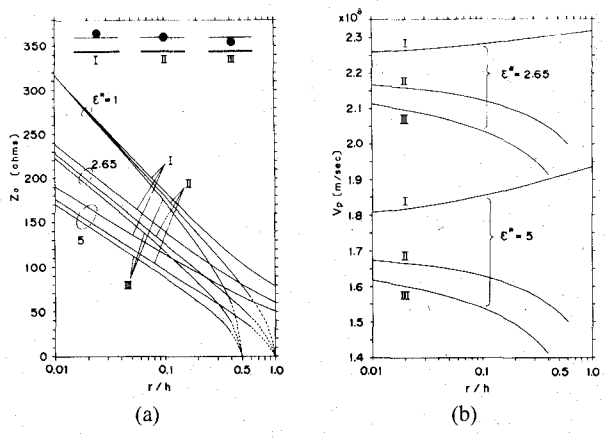

(a) (b)

Fig. 6. (a) Characteristic impedances and (b) phase velocities versus r/h.

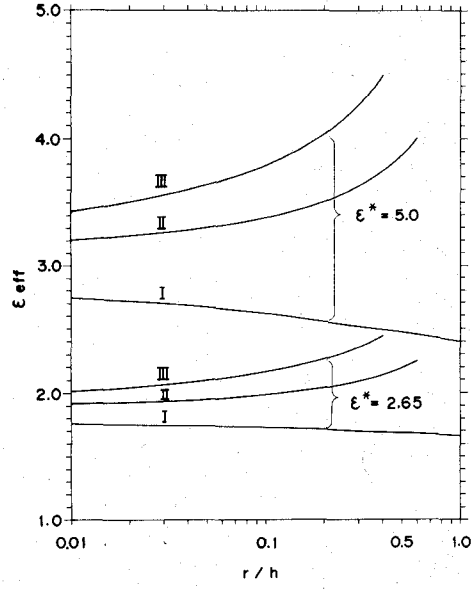

Fig. 7. Effective relative dielectric constants versus r/h.

is based on the fact that the potential error by the charge simulation method yields generally the maximum value at the middle point between the adjacent contour points on the conductor surface.

In Fig. 5(a), both F and the capacitance error are obviously reduced by increasing the number of charges. They are also reduced as r_q/r approaches zero. However, the later phenomenon is not always general [17]. Therefore, we use $r_q/r = 0.2$, after due consideration of the safety. Fig. 5(b) shows the capacitance error versus n for various r/h ratios when $r_q/r = 0.2$. In Fig. 5(b), the capacticance errors increase as r/h increases. Furthermore, Fig. 5(a) and (b) shows that the values of capacitance in this paper present the lower bounds, because this method is equivalent to dealing with the charge density on the wire surface. Fig. 5(c) shows the potential error on the wire surface of the structure with $r/h = 0.2$ and $H = h$ when $r_q/r = 0.2$ and $n = 9$. In Fig. 5(c), there is no notable difference in the distributed potential errors for $\epsilon^* = 1.0$, 2.65, or 5.0. It can be concluded that the capacitance errors, as well as the values of F for $\epsilon^* = 2.65$ and 5.0, are almost the same as those for $\epsilon^* = 1.0$. Therefore, we can investigate the accuracy of the capacitance by inspecting the potential error on the wire surface.

IV. Graphical Presentation of Z_0 and v_p, and an Approximate Formula

The parameters, a characteristic impedance Z_0 and a phase velocity v_p, for the structures shown in Fig. 2 can be obtained from the line capacitance as follows:

$$Z_0 = 1/v_0 C_0 \sqrt{\epsilon_{\text{eff}}} \tag{7}$$

$$v_p = v_0/\sqrt{\epsilon_{\text{eff}}} \tag{8}$$

where

$\epsilon_{\text{eff}} = C/C_0$ effective relative dielectric constant,

C_0 capacitance without adhesive ($\epsilon^* = 1.0$),

C capacitance with adhesive present, and

$v_0 = 2.997925 \times 10^8$ (m/s) velocity of light in free-space,

assuming quasi-static TEM propagation. The characteristics are presented here in graphical form for each of three cases of (I) $H = h + r$, (II) $H = h$, and (III) $H = h - r$. Then, we use the number of charges n and the arrangement of charges r_q/r as follows:

$$\left.\begin{matrix} n = 9 \\ r_q/r = 0.2 \end{matrix}\right\}. \tag{9}$$

Fig. 6(a) shows the characteristic impedances of three structures as a function of r/h for $\epsilon^* = 1.0$, 2.65, and 5.0. Fig. 6(b) shows the corresponding phase velocities. In Fig. 6(a), Z_0 for case (I) approaches zero in the limit when r/h approaches infinity. However, cases (II) and (III) are quite different from case (I). Z_0, for cases (II) and (III), is zero when $r/h = 1.0$ and 0.5, respectively. In Fig. 6(b), v_p, for case (I), increases as r/h increases. However, those for cases (II) and (III) decrease. Fig. 7 shows the corresponding effective relative dielectric constants ϵ_{eff}.

From the results of Fig. 6, we obtain a useful approximate formula of Z_0 for the structure with $\epsilon^* = 5.0$ of case

(II). That is

$$Z_0 = 17.08 + 34.83 \ln \frac{h}{r}, \qquad \text{for } \epsilon^* = 5.0,\ 0.01 \leqslant \frac{r}{h} \leqslant 0.3. \tag{10}$$

The errors of this formula are within 0.35 percent when compared to the data of Fig. 6(a). Furthermore, the differences between the present formula and the experiment [3] are about 2 (Ω) for the wire of $2r = 0.16$ (mm).

V. Conclusion

The characteristic impedances and the phase velocities of MWB's have been presented in graphical form for three analytical structures. An approximate formula which is useful for design of MWB's has also been presented.

Acknowledgment

The authors would like to thank K. Kamata and T. Hara at Ibaraki Technical College for helpful discussions, and Dr. H. Kamiyama at Simodate Research Laboratory, Hitachi Chemical Co., Ltd., for providing the available literature, and the reviewers for helpful suggestions which have improved the readability of the paper.

References

[1] R. P. Burr and R. J. Keogh, "A new simplified approach to high density interconnections," in *Proc. NEPCON'70 WEST.*

[2] N. Fukutomi and M. Asai, "Multiwire—New technology of printed wiring board," *Trans. IECE of Japan*, CPM-74-61, pp. 49–58, 1974 (in Japanese).

[3] E. Sugita, O. Ibaragi, T. Takei, and K. Aoki, "Electrical characteristics of multiwire circuit board," *Trans. IECE of Japan*, CPM76-80, pp. 15–22, 1976 (in Japanese).

[4] E. Sugita and O. Ibaragi, "Reliable multiwire circuits with small gauge wires," *IEEE Trans. Components, Hybrids, Manuf. Technol.*, vol. CHMT-2, pp. 532–536, Dec. 1979.

[5] H. R. Kaupp, "Characteristics of microstrip transmission lines," *IEEE Trans. Electron. Comp.*, vol. EC-16, pp. 185–193, Apr. 1967.

[6] H. Kaden, "Leitungs-und Kopplungskonstanten bei Streifenleitungen," Arch. Elek. Ubertragung., Heft 3, Band 21, pp. 109–111, 1967.

[7] M. A. R. Gunston, *Microwave Transmission Line Impedance Data.* London: Van Nostrand-Reinhold, 1972.

[8] H. A. Wheeler, "Transmission-line properties of a strip on a dielectric sheet on a plane," *IEEE Trans. Microwave Theory Tech.*, vol. MTT-25, pp. 631–647, Aug. 1977.

[9] H. A. Wheeler, "Transmission-line properties of a round wire in a polygon shield," *IEEE Trans. Microwave Theory Tech.*, vol. MTT-27, pp. 717–721, Aug. 1979.

[10] P. Silvester, "TEM wave properties of microstrip transmission lines," *Proc. Inst. Elec. Eng.*, vol. 115, pp. 43–48, Jan. 1968.

[11] W. T. Weeks, "Calculation of coefficients of capacitance of multiconductor transmission lines in the presence of a dielectric interface," *IEEE Trans. Microwave Theory Tech.*, vol. MTT-18, pp. 35–43, Jan. 1970.

[12] M. K. Krage and G. I. Haddad, "Characteristics of coupled microstrip transmission lines-II: Evaluation of coupled-line parameters," *IEEE Trans. Microwave Theory Tech.*, vol. MTT-18, pp. 222–228, Apr. 1970.

[13] K. Atsuki and E. Yamashita, "Analytical method for transmission lines with thick-strip conductor, multi-dielectric layers, and shielding conductor," *Trans. IECE of Japan*, vol. 53-B, pp. 322–328, June 1970 (in Japanese).

[14] H. Singer, H. Steinbigler, and P. Weiss, "A charge simulation method for the calculation of high voltage fields," *IEEE Trans. Power Apparatus Syst.*, vol. PAS-93, pp. 1660–1668, 1974.

[15] H. Shibata, S. Minakawa, and R. Terakado, "A numerical calculation of the capacitance for the rectangular coaxial line with offset inner conductor having an anisotropic dielectric," *IEEE Trans. Microwave Theory Tech.*, vol. MTT-31, pp. 385–391, May 1983.

[16] S. Murashima, M. Kato, and E. Miyachika, "On the property of the error in the charge simulation method," *Trans. IEE of Japan*, vol. 98-A, pp. 39–46, Jan. 1978 (in Japanese).

[17] S. Murashima, H. Kondo, M. Yokoi, and H. Nieda, "Relation between the error of the charge simulation method and the location of charges," *Trans. IEE of Japan*, vol. 102-A, pp. 1–8, Jan. 1982 (in Japanese).

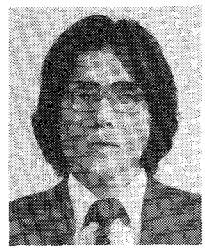

Hisashi Shibata was born in Takahagi, Ibaraki, Japan, on February 5, 1950. He received the B.E. degree in electrical engineering from Ibaraki University, Ibaraki, Japan, in 1975.

He joined the Department of Electrical Engineering, Ibaraki Technical College, Katsuta, Ibaraki, Japan, in 1975, where he is now an Associate Professor. His current research interests are the analysis of electromagnetic fields in an anisotropic medium and the applications of the theory to the microwave devices.

Mr. Shibata is a member of the Institute of Electrical Engineers of Japan, and the Institute of Electronics and Communication Engineers of Japan.

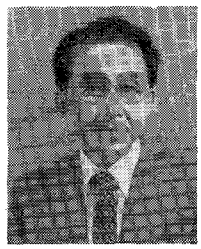

Ryuiti Terakado was born in Tokyo, Japan, on January 30, 1930. He graduated from the Taga Technical College, Ibaraki, Japan, in 1950. He received the D.E. degree from the Tokyo Institute of Technology, Tokyo, Japan, in 1975.

In 1960, he joined the Department of Electrical Engineering, Ibaraki University, where he is now a Professor. He is also a part-time lecturer at Ibaraki Technical College. His major research interests are two-dimensional fields and symmetry.

Dr. Terakado is a member of the Institute of Electrical Engineers, the Institute of Electronics and Communication Engineers, and the Society of Instrument and Control Engineers, all of Japan.